IET Control Theory & Applications

Adaptive control of quadrotor suspended load systems with variable payload and wind disturbances

Ruiying Wang[1] | Jun Shen[1] | Hongling Qiu[1] | Bohao Zhu[2]

[1]College of Automation Engineering, Nanjing University of Aeronautics and Astronautics, Nanjing, China

[2]Department of Mechanical Engineering, The University of Hong Kong, Hong Kong, Hong Kong

Correspondence
Bohao Zhu, Department of Mechanical Engineering, The University of Hong Kong, Pokfulam Road 999077, Hong Kong.
Email: zhubohao9374@gmail.com

Abstract
This paper introduces an adaptive control scheme for quadrotor suspended load systems, to track desired trajectory with variable payload and wind disturbances. The dynamic model of the quadrotor suspended load system is developed, taking into account the impact of the wind field described by the Dryden model. To attenuate the effects of payload variation and wind disturbances on the system, an adaptive control method based on disturbance observers is devised. Additionally, the uniform boundedness of all error signals is demonstrated. The effectiveness of the designed control method is verified through simulations, which serves to strengthen its applicability in practical applications.

1 | INTRODUCTION

The research and application of quadrotors have developed rapidly over the last few decades. Payload transportation is one of the most important application areas [1–3]. While the traditional method is to place the payload in the cargo hold, the cable-suspended configuration of the payload has also been widely investigated in recent years. Cable-suspended payloads offers several advantages, including larger payload capacity for quadrotors, no effect on quadrotor inertia [4], high cost effectiveness [5], and so on. In particular, in regions lacking suitable landing areas, such as lakes and mountainous areas, quadrotor suspended payload systems provide a convenient and efficient way to transport cargo. In order to further improve the load capacity of quadrotors, researchers have conducted a lot of studies on quadrotor suspended load systems.

The challenges in controller design for quadrotor suspended load systems are attributed to the underactuated nature of the system, which has eight degrees of freedom but only four control inputs. In addition, the control design is further complicated by the nonlinear and coupled nature of the system. To address these challenges, researchers have proposed various control strategies. In [6], a partial feedback linearized control method was used to control the system in the $x - z$ plane. Passive controllers were developed in [7] specifically designed for the system. An interconnection and damping distribution controller was proposed in [8]. Considering the coupled dynamics of the system, a geometric PID controller was constructed in [9] using a coordinate-free form. In [10], a nonlinear backstepping controller was designed. The operation of the system was divided into three phases: setup, pull, and raise, and controllers were developed for each phase to ensure effective control in [11]. These approaches aim to enhance control performance and effectively handle nonlinearity and underactuation. However, these methods are mainly aimed at the ideal control of a specific system and do not fully take into account the effects of unknown parameter variations and external disturbances.

Due to the wide range of payloads carried by suspended load quadrotors, the controller is often affected by payload uncertainties. These uncertainties include variations in parameters such as the weight, shape, size, and center of gravity of the suspended payload. To address these parameter uncertainties, researchers have employed various methods to improve control performance. Current approaches primarily focus on adaptive control techniques. In [12], an adaptive tracking controller was added to the geometric controller to address the problem of unknown quadrotor inertia. In [13], the controller of quadrotors was designed by combining the backstepping

control and adaptive control to solve the problem of parameter uncertainties. In addition, in [14], sliding mode control (SMC) and backstepping control were combined with adaptive control for estimating varying loads. In [15], an adaptive controller based on the energy principle was developed for the case of uncertainty in the cable length. Furthermore, in [16], an adaptive controller and passive based backstepping controller were designed for underactuated hybrid quadrotors, where adaptive control is used to estimate the uncertain parameters of quadrotors. These works have demonstrated the potential of the system to transport varying payloads.

External disturbances impact the stability of the quadrotor suspended load system, and a lot of work has been done to improve the resistance to disturbances of the system. In [17], the robustness of SMC was exploited to mitigate the adverse effects caused by disturbances on quadrotors. Furthermore, in [18], a nonlinear disturbance observer was designed to estimate disturbances. In [19], an adaptive sliding mode disturbance observer was used to estimate external disturbances. In [20], extended state observers were used to monitor external disturbances. However, all of the above work models external disturbances as simple sinusoidal functions. In real-life scenarios, real disturbances are often complex and unpredictable. For instance, quadrotors are subjected to a variety of wind conditions, including different wind speeds, wind directions, and airflow characteristics due to factors such as sudden turbulence, atmospheric inhomogeneities, and the presence of surrounding structures. The uncertainty and instability of the wind can significantly impact the attitude stability, flight trajectory, and load capacity of the quadrotor, posing a significant challenge to designing the quadrotor controller.

To better simulate complex wind disturbances, this paper introduces the Dryden model [21]. The Dryden model is a commonly used aerodynamic model that accurately describes the dynamic characteristics of the wind field [22]. It requires detailed modelling of the wind speed power spectral density to reflect the wind dynamic changes. Due to the higher irregularities and complexity of the wind disturbances simulated by the Dryden model, more robust controllers must be designed. In addition, real-time estimation and compensation of complex wind disturbances is a key condition to ensure that the system exhibits robustness, which requires the design of more accurate disturbance observers.

Inspired by the above literature, this paper presents an adaptive control method based on disturbance observers to address the impact of payload mass variations and wind disturbances on quadrotor suspended load systems. This paper contributes in the following aspects:

1. Compared with [12–16], which only considers model parameter changes or external disturbances, this paper comprehensively considers the effects of payload mass variations and wind disturbances on the quadrotor suspended load system. The proposed control strategies are closer to practical application scenarios.
2. Unlike [17–20] which adopts sinusoidal function or constant value to simulate external disturbances, this paper intro-
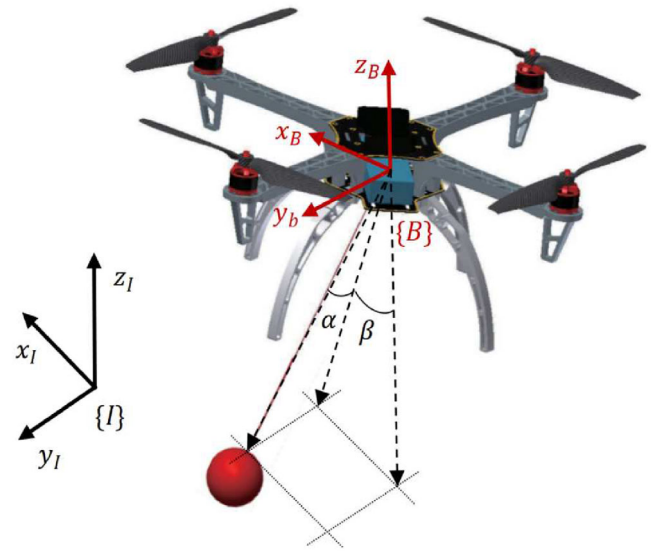

FIGURE 1 Schema of the quadrotor suspended load system.

duces the Dryden model. The Dryden model can simulate the stochastic rise and fall of the wind speed, and can reflect more accurately the natural state of the wind, which makes the description of wind disturbances closer to the real situation.

3. In contrast to [12–15], this paper introduces a convergence term in the adaptive control law for mass estimation. In addition, unlike [18, 19] that assumed the disturbance derivative to be zero, this paper imposes upper and lower bounds on the disturbance derivative. Based on this, a stability analysis of the closed-loop system is provided, and it is demonstrated that the control scheme ensures that all error signals are uniform boundedness.

This paper is structured as follows: Section 2 introduces the model of quadrotor suspended payload system and the Dryden model. In Section 3, an adaptive controller based on disturbance observers is designed. The uniform boundedness of all error signals is demonstrated in Section 4. Simulations are conducted in Section 5. Finally, Section 6 presents the conclusions.

2 | DYNAMIC MODEL

2.1 | Dynamic model of the quadrotor suspended load system

To describe the flight motion of the quadrotor suspended load system, two coordinate systems are established: the inertial frame $I = \{x_I, y_I, z_I\}$ and the body coordinate frame $B = \{x_B, y_B, z_B\}$. The system schematic is depicted in Figure 1.

The associated generalized coordinate is represented by the vector $q = [\xi^T, \sigma^T, \eta^T]^T$, where $\xi = [x, y, z]^T \in \mathbb{R}^3$ represents the position vector of the quadrotor, $\eta = [\phi, \theta, \psi]^T \in \mathbb{R}^3$ represents the attitude of the quadrotor, $\sigma = [\alpha, \beta]^T \in \mathbb{R}^2$ represents the swing angles of the payload.

The rotation matrix from B to I is described by

$$R_B^I = \begin{bmatrix} \cos\theta\cos\psi & -\cos\phi\sin\psi + \sin\phi\sin\theta\cos\psi & \sin\theta\sin\psi + \cos\phi\sin\theta\cos\psi \\ \cos\theta\sin\psi & \cos\phi\cos\psi + \sin\phi\sin\theta\sin\psi & -\sin\theta\cos\psi + \cos\phi\sin\theta\sin\psi \\ -\sin\theta & \sin\phi\cos\theta & \cos\phi\cos\theta \end{bmatrix}.$$

The torque generated by the quadrotor in the inertial frame is denoted as $\tau = [\tau_\phi, \tau_\theta, \tau_\psi]^T \in \mathbb{R}^3$. The total thrust generated by the quadrotor is denoted by T. Then, the thrust vector is denoted as $U = [U_x, U_y, U_z] \in \mathbb{R}^3$ in the inertial frame, which is specified as:

$$U = \begin{bmatrix} U_x \\ U_y \\ U_z \end{bmatrix} = T \begin{bmatrix} \sin\theta\sin\psi + \cos\phi\sin\theta\cos\psi \\ -\sin\theta\cos\psi + \cos\phi\sin\theta\sin\psi \\ \cos\phi\cos\theta \end{bmatrix}.$$

The position vector of the payload $\xi_L = [x_L, y_L, z_L]^T \in \mathbb{R}^3$ is denoted by

$$\begin{cases} x_L = x + l\sin\beta, \\ y_L = y + l\cos\beta\sin\alpha, \\ z_L = z - l\cos\beta\cos\alpha, \end{cases} \tag{1}$$

where l is the length of the cable.

Before deriving the mathematical model of the system, the following assumptions are made.

Assumption 1. The mass of the cable is ignored and remains taut at all times.

Assumption 2. The suspension point coincides with the centre of gravity of the quadrotor.

Assumption 3. The attitude angles $\phi, \theta, \alpha, \beta \in (-\frac{\pi}{2}, \frac{\pi}{2}), \psi \in (-\pi, \pi)$.

The Euler–Lagrange equation is given as

$$\frac{\mathrm{d}}{\mathrm{d}t}\left(\frac{\partial L}{\partial \dot{q}}\right) - \frac{\partial L}{\partial q} = F. \tag{2}$$

The Lagrangian is given by

$$L = \frac{m_Q\left(\dot{x}^2 + \dot{y}^2 + \dot{z}^2\right)}{2} + \frac{m_L\left(\dot{x}_L^2 + \dot{y}_L^2 + \dot{z}_L^2\right)}{2} + \frac{I_x\omega_x^2 + I_y\omega_y^2 + I_z\omega_z^2}{2} - m_Q g z - m_L g z_L, \tag{3}$$

where $I = \mathrm{diag}(I_x, I_y, I_z) \in \mathbb{R}^{3\times3}$ represents quadrotor moment inertia, $\omega = [\omega_x, \omega_y, \omega_z]^T \in \mathbb{R}^3$ is angular velocity, the mass of the quadrotor and the payload are denoted by m_Q, m_L, the gravity acceleration is denoted by g.

The external generalized force $F \in \mathbb{R}^8$ in Equation (2) is divided into the generalized active force $F_a \in \mathbb{R}^8$ and the generalized wind drag force $F_w \in \mathbb{R}^8$ as

$$F = F_a + F_w. \tag{4}$$

Here, the generalized active force F_a generated by the rotor thrusts is expressed as

$$F_a = [U_x, U_y, U_z, 0, 0, \tau_\phi, \tau_\theta, \tau_\psi]^T.$$

The generalized drag force F_w is given by

$$F_w = [F_{wx}, F_{wy}, F_{wz}, F_{w\alpha}, F_{w\beta}, \tau_{w\phi}, \tau_{w\theta}, \tau_{w\psi}]^T.$$

Substituting Equations (1) and (3) into Equation (2), we can derive the dynamic model of the system [23],

$$M(q)\ddot{q} + C(q,\dot{q})\dot{q} + V_m(q) = F, \tag{5}$$

where $M(q) \in \mathbb{R}^{8\times8}$, $C(q,\dot{q}) \in \mathbb{R}^{8\times8}$, $V_m(q) \in \mathbb{R}^8$ are defined as

$$M(q) = \begin{bmatrix} M_{11} & M_{12} & 0_{3\times3} \\ M_{12}^T & M_{22} & 0_{3\times2} \\ 0_{3\times3} & 0_{2\times3} & I \end{bmatrix}, \quad C(q,\dot{q}) = \begin{bmatrix} 0_{3\times3} & m_L/C_1 & 0_{3\times3} \\ 0_{2\times3} & m_L/C_2 & 0_{2\times3} \\ 0_{3\times3} & 0_{3\times2} & C_3 \end{bmatrix},$$

$$V_m(q) = \begin{bmatrix} G_1 \\ G_2 \\ 0_{3\times1} \end{bmatrix},$$

with

$$M_{11} = \begin{bmatrix} m_Q + m_L & 0 & 0 \\ 0 & m_Q + m_L & 0 \\ 0 & 0 & m_Q + m_L \end{bmatrix},$$

$$M_{12} = \begin{bmatrix} 0 & m_L l\cos\beta \\ m_L l\cos\alpha\cos\beta & -m_L l\sin\alpha\sin\beta \\ m_L l\sin\alpha\cos\beta & m_L l\cos\alpha\sin\beta \end{bmatrix},$$

$$M_{22} = \begin{bmatrix} m_L l^2 \cos^2\theta & 0 \\ 0 & m_L l^2 \end{bmatrix}, \quad C_1 = \begin{bmatrix} 0 & -\sin\beta\dot\beta \\ -\sin\alpha\cos\beta\dot\alpha - \cos\alpha\sin\beta\dot\beta & -\cos\alpha\sin\beta\dot\alpha - \sin\alpha\cos\beta\dot\beta \\ -\cos\alpha\cos\beta\dot\alpha - \sin\alpha\sin\beta\dot\beta & -\sin\alpha\sin\beta\dot\alpha + \cos\alpha\cos\beta\dot\beta \end{bmatrix},$$

$$C_2 = \begin{bmatrix} -l\cos\beta\sin\beta\dot\beta & -l\cos\beta\sin\beta\dot\alpha \\ l\cos\beta\sin\beta\dot\alpha & 0 \end{bmatrix},$$

$$C_3 = \begin{bmatrix} 0 & \frac{I_y - I_z}{2}\dot\psi & \frac{I_y - I_z}{2}\dot\theta \\ \frac{I_z - I_x}{2}\dot\psi & 0 & \frac{I_z - I_x}{2}\dot\phi \\ \frac{I_x - I_y}{2}\dot\theta & \frac{I_x - I_y}{2}\dot\phi & 0 \end{bmatrix},$$

$$G_1 = \begin{bmatrix} 0 \\ 0 \\ (m_Q + m_L)g \end{bmatrix}, \quad G_2 = \begin{bmatrix} m_L lg\sin\alpha\cos\beta \\ m_L lg\cos\alpha\sin\beta \end{bmatrix}.$$

When the controller design is taken into consideration, the dynamic mode can be reformulated as

$$\begin{cases} \ddot\xi = \dfrac{U}{m_Q + m_L} - ge_3 - \dfrac{m_L la}{m_Q + m_L} + d_w\xi, \\ \ddot\sigma = M_{22}^{-1}(-M_{12}^T\ddot\xi - m_L l C_2\dot\sigma - G_2) + d_{w\sigma}, \\ \ddot\eta = I^{-1}(\tau - \dot\eta \times I\dot\eta) + d_{w\eta}, \end{cases} \tag{6}$$

where $d_w\xi = \dfrac{F_w\xi}{m_Q + m_L}$, $d_{w\sigma} = M_{22}^{-1}F_{w\sigma}$, $d_{w\sigma} = I^{-1}\tau_{w\eta}$, $a = [a_1, a_2, a_3]^T \in \mathbb{R}^3$, and

$$\begin{cases} a_1 = -\sin\beta\dot\beta^2 + \cos\beta\ddot\beta, \\ a_2 = -\cos\beta\sin\alpha\dot\beta^2 - 2\sin\beta\cos\alpha\dot\beta\dot\alpha - \cos\beta\sin\alpha\dot\alpha^2 \\ \qquad - \sin\beta\sin\alpha\ddot\beta + \cos\beta\cos\alpha\ddot\alpha, \\ a_3 = \cos\beta\cos\alpha\dot\beta^2 - 2\sin\beta\sin\alpha\dot\beta\dot\alpha + \cos\beta\cos\alpha\dot\alpha^2 \\ \qquad + \sin\beta\cos\alpha\ddot\beta + \cos\beta\sin\alpha\ddot\alpha. \end{cases}$$

Disturbance vectors $F_w\xi = [F_{wx}, F_{wy}, F_{wz}]^T \in \mathbb{R}^3$, $F_{w\sigma} = [F_{w\alpha}, F_{w\beta}]^T \in \mathbb{R}^2$, and $\tau_{w\eta} = [\tau_{w\phi}, \tau_{w\theta}, \tau_{w\psi}]^T \in \mathbb{R}^3$, will be quantified using the Dryden model described in the next section. In Equation (6), the system parameter m_L changes with payload variation.

2.2 | The Dryden model

All types of wind can affect the velocity and angular velocity of the quadrotor, thereby changing the output force and torque of the quadrotor. In this paper, the Dryden model is used to simulate wind disturbances [24].

The turbulence intensities $\sigma_u, \sigma_v, \sigma_w$ are expressed as

$$\sigma_w = 0.1u_0,$$

$$\frac{\sigma_u}{\sigma_w} = \frac{\sigma_v}{\sigma_u} = \frac{1}{(0.177 + 0.000823h_0)^{0.4}},$$

where h_0 is the altitude of the quadrotor and u_0 is the wind speed at the height of 6.096 m.

The turbulence scales are expressed as

$$2L_w = h_0,$$

$$L_u = 2L_v = \frac{h}{(0.177 + 0.000823h_0)^{1.2}}.$$

The spectral density function $\Phi_u(\omega_t)$, $\Phi_v(\omega_t)$, $\Phi_w(\omega_t)$, $\Phi_p(\omega_t)$, $\Phi_q(\omega_t)$, and $\Phi_r(\omega_t)$ of the Dryden model are expressed as

$$\Phi_u(\omega_t) = \sigma_u^2 \frac{L_u}{\pi V}\frac{1}{1 + \left(L_u\frac{\omega_t}{V}\right)^2}, \quad \Phi_v(\omega_t) = \sigma_v^2 \frac{L_v}{\pi V}\frac{1 + 12\left(L_v\frac{\omega_t}{V}\right)^2}{\left[1 + 4\left(L_v\frac{\omega_t}{V}\right)^2\right]^2},$$

$$\Phi_w(\omega_t) = \sigma_w^2 \frac{L_w}{\pi V}\frac{1 + 12\left(L_w\frac{\omega_t}{V}\right)^2}{\left[1 + 4\left(L_w\frac{\omega_t}{V}\right)^2\right]^2},$$

$$\Phi_p(\omega_t) = \frac{\sigma_w^2}{L_w V}\frac{0.4\left(\frac{\pi L_w}{2r}\right)^{\frac{1}{3}}}{1 + \left(\frac{4r\omega_t}{\pi V}\right)^2}, \quad \Phi_q(\omega_t) = \left(\frac{\omega_t}{V}\right)^2\frac{\Phi_v(\omega_t)}{1 + \left(\frac{3r\omega_t}{\pi V}\right)^2},$$

$$\Phi_r(\omega_t) = \left(\frac{\omega_t}{V}\right)^2\frac{\Phi_w(\omega_t)}{1 + \left(\frac{4r\omega_t}{\pi V}\right)^2}, \tag{7}$$

where ω_t is time frequency, V is the airspeed, and r is the quadrotor wheelbase.

White noise signal $n(t)$ is passed through filters with transfer function $G(s)$, to obtain output sequence $x(t)$. The spectrum functions $\Phi(\omega_t)$ of the output sequence $x(t)$ is as follows:

$$\Phi(\omega_t) = |G(i\omega_t)|^2 = G^*(i\omega_t)(i\omega_t).$$

Using the above equation to decompose Equation (7), the transfer function of the filters can be obtained as

$$G_u(s) = \frac{K_u}{T_u s + 1}, \quad G_w(s) = \frac{K_w}{T_w s + 1}, \quad G_v(s) = \frac{K_v}{T_v s + 1},$$

$$G_p(s) = \frac{K_p}{T_p s + 1}, \quad G_q(s) = \frac{K_q}{T_q s + 1} G_w(s), \quad G_r(s) = \frac{K_r}{T_r s + 1} G_v(s),$$

(8)

where $K_u = \sigma_u \sqrt{L_u/\pi V}$, $T_u = L_u/V$, $K_v = \sigma_v \sqrt{L_v/\pi V}$, $T_v = 2L_v/\sqrt{3}V$, $K_w = \sigma_w \sqrt{L_w/\pi V}$, $T_w = 2L_w/\sqrt{3}V$, $K_p = \sigma_w \sqrt{\frac{0.4}{L_w V}} (\frac{\pi L_w}{2r})^{\frac{1}{3}}$, $T_p = 4r/\pi V$, $K_q = 1/V$, $T_q = 4r/\pi V$, $K_r = 1/V$, $T_r = 3r/\pi V$.

White noise signal can be converted to wind velocity disturbance $V_{\text{wind}} = [V_x, V_y, V_z]^T$ and wind direction disturbance $\omega_{\text{wind}} = [\omega_\phi, \omega_\theta, \omega_\psi]^T$ using the above filters.

The wind drag forces are approximated as a linear function of the wind speed, as suggested in [25] and [26]. The generalized wind drag forces can be expressed by the following equation,

$$F_{wx} = \lambda_{11} V_x^2, \quad F_{wy} = \lambda_{12} V_y^2, \quad F_{wz} = \lambda_{13} V_z^2,$$

$$F_{w\alpha} = \lambda_{21} \sqrt{V_y^2 + V_z^2},$$

$$F_{w\beta} = \lambda_{22} \sqrt{V_x^2 + V_z^2}, \quad \tau_{w\phi} = \lambda_{31} \omega_\phi^2, \quad \tau_{w\theta} = \lambda_{32} \omega_\theta^2,$$

$$\tau_{w\psi} = \lambda_{33} \omega_\psi^2,$$

(9)

where $\lambda_{11}, \lambda_{12}, \lambda_{13}, \lambda_{21}, \lambda_{22}, \lambda_{31}, \lambda_{32}, \lambda_{33}$ are wind drag coefficients.

3 | CONTROLLER DESIGN

In this section, position controller and attitude controller are designed. An adaptive law is introduced to estimate and compensate for variable payload. Additionally, disturbance observers are used to estimate and counteract the impact of wind disturbance. The system control structure is shown in Figure 2.

3.1 | Adaptive controller

The tracking errors of the quadrotor are defined as [27]

$$\begin{cases} e_{\xi 1} = \xi_d - \xi, \\ e_{\xi 2} = \dot{\xi}_d - \dot{\xi} + c_1 e_{\xi 1}, \end{cases}$$

(10)

$$\begin{cases} e_{\eta 1} = \eta_d - \eta, \\ e_{\eta 2} = \dot{\eta}_d - \dot{\eta} + c_2 e_{\eta 1}, \end{cases}$$
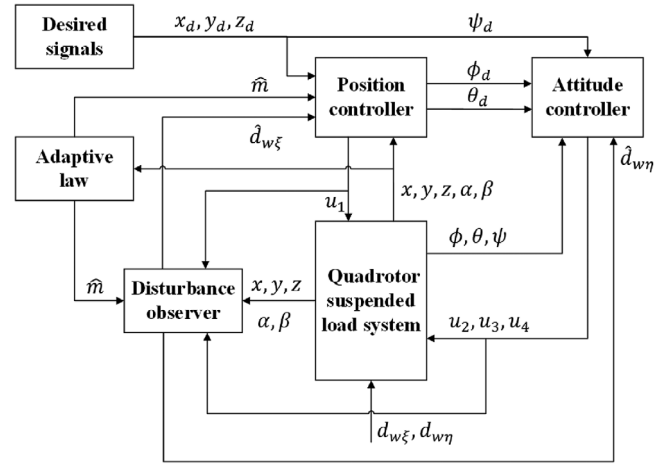
(11)

FIGURE 2 The system control structure.

where $c_1 = \text{diag}(c_{11}, c_{12}, c_{13})$, $c_2 = \text{diag}(c_{21}, c_{22}, c_{23})$ are positive definite, $\xi_d = [x_d, y_d, z_d]^T$, $\eta_d = [\phi_d, \theta_d, \psi_d]^T$ are the desired trajectory of position and attitude.

Take the position and attitude controllers as

$$\begin{cases} U = (m_Q + m_L)\left(\ddot{\xi}_d + (c_1 + k_1)e_{\xi 2} + e_{\xi 1} - c_1^T c_1 e_{\xi 1} + g e_3 - d_\xi\right) + m_L la, \\ \tau = I\left(\ddot{\eta}_d + (c_2 + k_2)e_{\eta 2} + e_{\eta 1} - c_2^T c_2 e_{\eta 1} - d_\eta\right) + \dot{\eta} \times I\dot{\eta}, \end{cases}$$

(12)

where $k_1 = \text{diag}(k_{11}, k_{12}, k_{13})$, $k_2 = \text{diag}(k_{21}, k_{22}, k_{23})$ are positive definite.

Considering that the payload mass m_L is unknown, it is estimated using an adaptive law which is

$$\dot{\hat{m}}_L = \gamma_1 e_{\xi 2}^T (\bar{U} + la) - \gamma_2 \hat{m}_L (\bar{U} + la)^T (\bar{U} + la),$$

(13)

where γ_1 and γ_2 are positive constants, $\hat{m}_L$ is the estimation of m_L, and

$$\bar{U} = \ddot{\xi}_d + k_1 e_{\xi 2} + c_1(e_{\xi 2} + c_1 e_{\xi 1}) + g e_3.$$

The estimation error is defined as

$$\tilde{m}_L = m_L - \hat{m}_L.$$

Note that m is a constant, it follows that $\dot{\tilde{m}}_L = -\dot{\hat{m}}_L$.

Combining this adaptive law (13), the new controller is obtained as

$$\begin{cases} U = (m_Q + \hat{m}_L)\left(\ddot{\xi}_d + (c_1 + k_1)e_{\xi 2} + e_{\xi 1} - c_1^T c_1 e_{\xi 1} + g e_3 - d_\xi\right) + \hat{m}_L la, \\ \tau = I\left(\ddot{\eta}_d + (c_2 + k_2)e_{\eta 2} + e_{\eta 1} - c_2^T c_2 e_{\eta 1} - d_\eta\right) + \dot{\eta} \times I\dot{\eta}. \end{cases}$$

(14)

Remark 1. The adaptive law proposed in this paper increases the convergence term, which can significantly improve the estimation accuracy for the payload mass, and enhance the robustness of the system. In subsequent simulations, the advantage of the adaptive law with convergence term is further shown.

3.2 | Disturbance observers

Assumption 4. The wind disturbances satisfy $| \dot{d}_\xi | \leq E_{w\xi}$ and $| \dot{d}_\eta | \leq E_{w\eta}$.

The disturbance observers are designed as [28]

$$
\begin{cases}
\hat{d}_{w\xi} = z_\xi + p(\xi), \\
\dot{z}_\xi = -k_3 z_\xi - k_3 \left(\dfrac{U}{m_Q + \hat{m}_L} - ge_3 - \dfrac{\hat{m}_L la}{m_Q + \hat{m}_L} + p(\xi) \right),
\end{cases}
\tag{15}
$$

$$
\begin{cases}
\hat{d}_{w\eta} = z_\eta + p(\eta), \\
\dot{z}_\eta = -k_4 z_\eta - k_4 \left(I^{-1}(\tau - \dot{\eta} \times I\dot{\eta}) + p(\eta) \right),
\end{cases}
\tag{16}
$$

where z_ξ and z_η are the internal states of the observers, $k_3 = \text{diag}(k_{31}, k_{32}, k_{33})$ and $k_4 = \text{diag}(k_{41}, k_{42}, k_{43})$ are positive definite, $p(\xi) = k_3 \dot{\xi}$, $p(\eta) = k_4 \dot{\eta}$.

Remark 2. Adaptive disturbance observers are often used when external disturbance is present. However, these methods often lack accuracy when dealing with irregular disturbances. To overcome this challenge, the nonlinear disturbance observer in [28] is used in this paper. This disturbance observer uses the reference model of the system, which performs better than other methods when dealing with rapidly changing and irregular disturbances. Moreover, for the quadrotor suspended load system with an unknown payload mass, we improved the performance of disturbance observers by introducing an adaptive law, which was not addressed in [28]. In subsequent simulations, the advantages of the designed disturbance observer in dealing with wind disturbances and payload variations are further demonstrated.

With the estimations of wind disturbances $\hat{d}_\xi$ and $\hat{d}_\eta$, the wind disturbance estimation errors are defined as

$$
\begin{cases}
\tilde{d}_{w\xi} = d_{w\xi} - \hat{d}_{w\xi}, \\
\tilde{d}_{w\eta} = d_{w\eta} - \hat{d}_{w\eta}.
\end{cases}
\tag{17}
$$

Recalling the control law (14) presented in the previous subsection, based on the disturbance observers, the parameters $d_{w\xi}$, $d_{w\eta}$ in Equation (14) are replaced by $\hat{d}_{w\xi}$, $\hat{d}_{w\eta}$, the control law is reformulated in the following:

$$
\begin{cases}
U = (m_Q + \hat{m}_L)\left(\ddot{\xi}_d + (c_1 + k_1)e_{\xi 2} + e_{\xi 1} - c_1^T c_1 e_{\xi 1} + ge_3 - \hat{d}_{w\xi} \right) + \hat{m}_L la, \\
\tau = I\left(\ddot{\eta}_d + (c_2 + k_2)e_{\eta 2} + e_{\eta 1} - c_2^T c_2 e_{\eta 1} - \hat{d}_{w\eta} \right) + \dot{\eta} \times I\dot{\eta},
\end{cases}
\tag{18}
$$

where $\hat{m}_L$, $\hat{d}_{w\xi}$, $\hat{d}_{w\eta}$ are given in Equations (13), (15), and (16).

In addition, the desired trajectory ξ_d and the desired yaw angle ψ_d are given according to the specific requirements of the mission. Due to the underactuation and coupled nature of quadrotor suspended load systems, the desired attitude θ_d and ϕ_d are determined using the position information, which are specified as:

$$
\phi_d = \arcsin \left(U_y \cos \psi - U_x \sin \psi \right),
$$

$$
\theta_d = \arcsin \frac{-U_y \sin \psi - U_x \cos \psi}{\cos \phi_d}.
$$

4 | STABILITY ANALYSIS

Theorem 1. *Consider the quadrotor suspended load system (6) with Assumptions 1–4, the controller is given by Equation (14), the adaptive law is given by Equation (13), and the disturbance observers are given by Equations (15) and (16). If the control parameters satisfy that $k_{1i} > \frac{1}{2}$, $k_{2i} > \frac{1}{2}$, $k_{3i} > M$, $k_{4i} > 1$ $(i = 1, 2, 3)$, and $\gamma > 1$, then there exists t' such that the error $e = e_{\xi 1}^T e_{\xi 1} + e_{\xi 2}^T e_{\xi 2} + e_{\eta 1}^T e_{\eta 1} + e_{\eta 2}^T e_{\eta 2} + \frac{\tilde{m}_L}{\gamma_1(m_Q + m_L)} + \tilde{d}_{w\xi}^T \tilde{d}_{w\xi} + \tilde{d}_{w\eta}^T \tilde{d}_{w\eta}$ satisfies $e(t) \leq \frac{2b}{a}$ when $t > t'$, where*

$$
a = \min_{i \in \{1,2,3\}} \min \left\{ c_{1i}, c_{2i}, k_{1i} - \frac{1}{2}, k_{2i} - \frac{1}{2}, k_{3i} - M, k_{4i} - 1, \frac{K(\gamma - 1)}{2} \right\},
$$

$$
b = \frac{K\gamma}{2} m_L^2 + \frac{E_{w\xi}^2}{2} + \frac{E_{w\eta}^2}{2},
$$

$$
M = 1 + \frac{1}{2(m_Q + m_L)}, \quad K = \frac{(\bar{U} + la)^T (\bar{U} + la)}{m_Q + m_L}, \quad \gamma = \frac{\gamma_2}{\gamma_1}, \text{ and } I \text{ is an}
$$

identity matrix.

Proof. Construct the Lyapunov candidate function as:

$$
V_1 = \frac{1}{2} e_{\xi 1}^T e_{\xi 1} + \frac{1}{2} e_{\xi 2}^T e_{\xi 2} + \frac{1}{2} e_{\eta 1}^T e_{\eta 1} + \frac{1}{2} e_{\eta 2}^T e_{\eta 2} + \frac{1}{2\gamma_1(m_Q + m_L)} \tilde{m}_L^2.
$$

Considering Equations (10), (11), (14), (13), (15), and (16), it can be deduced that

$$
\dot{e}_{\xi 1} = e_{\xi 2} - c_1 e_{\xi 1},
$$

$$
\dot{e}_{\xi 2} = -e_{\xi 1} - k_1 e_{\xi 2} + \frac{\tilde{m}_L(\bar{U} + la)}{m_Q + m_L} - \tilde{d}_{w\xi},
$$

$$
\dot{e}_{\eta 1} = e_{\eta 2} - c_2 e_{\eta 1},
$$

$$
\dot{e}_{\eta 2} = -e_{\eta 1} - k_2 e_{\eta 2} - \tilde{d}_{w\eta}.
$$

The time derivative of V_1 is given by

$$
\dot{V}_1 = e_{\xi 1}^T \dot{e}_{\xi 1} + e_{\xi 2}^T \dot{e}_{\xi 2} + e_{\eta 1}^T \dot{e}_{\eta 1} + e_{\eta 2}^T \dot{e}_{\eta 2} + \frac{1}{\gamma_1(m_Q + m_L)} \tilde{m}_L \dot{\tilde{m}}_L
$$

$$
= e_{\xi 1}^T (e_{\xi 2} - c_1 e_{\xi 1}) + e_{\xi 2}^T \left(-e_{\xi 1} - k_1 e_{\xi 2} + \frac{\tilde{m}_L(\bar{U} + la)}{m_Q + m_L} - \tilde{d}_{w\xi} \right)
$$

$$
+ e_{\eta 1}^T (e_{\eta 2} - c_2 e_{\eta 1}) + e_{\eta 2}^T (-e_{\eta 1} - k_2 e_{\eta 2} - \tilde{d}_{w\eta})
$$

$$
- \frac{1}{\gamma_1(m_Q + m_L)} \tilde{m}_L \left(\gamma_1 e_{\xi 2}^T (\bar{U} + la) - \gamma_2 \hat{m}_L (\bar{U} + la)^T (\bar{U} + la) \right)
$$

$$
= -e_{\xi 1}^T c_1 e_{\xi 1} - e_{\xi 2}^T k_1 e_{\xi 2} - e_{\eta 1}^T c_2 e_{\eta 1} - e_{\eta 2}^T k_2 e_{\eta 2} - e_{\xi 2}^T \tilde{d}_{w\xi} - e_{\eta 2}^T \tilde{d}_{w\eta}
$$

$$+ \frac{\gamma_2 \tilde{m}_L \hat{m}_L (\bar{U} + la)^T (\bar{U} + la)}{\gamma_1 (m_Q + m_L)}.$$

Construct the Lyapunov candidate function as:

$$V_2 = \frac{1}{2} \tilde{d}_{w\xi}^T \tilde{d}_{w\xi} + \frac{1}{2} \tilde{d}_{w\eta}^T \tilde{d}_{w\eta}.$$

Considering Equations (15)–(17), it can be deduced that

$$\dot{\tilde{d}}_{w\xi} = \dot{d}_{w\xi} - \dot{\hat{z}}_\xi - \dot{p}(\xi) = d_{w\xi} - k_3 \tilde{d}_{w\xi} + \frac{\tilde{m}_L (\bar{U} + la)}{m_Q + m_L},$$

$$\dot{\tilde{d}}_{w\eta} = \dot{d}_{w\eta} - \dot{\hat{z}}_\eta - \dot{p}(\eta) = d_{w\eta} - k_4 \tilde{d}_{w\eta}.$$

The time derivative of V_2 is given by

$$\dot{V}_2 = \tilde{d}_{w\xi}^T \dot{\tilde{d}}_{w\xi} + \tilde{d}_{w\eta}^T \dot{\tilde{d}}_{w\eta}$$

$$= -\tilde{d}_{w\xi}^T k_3 \tilde{d}_{w\xi} - \tilde{d}_{w\eta}^T k_4 \tilde{d}_{w\eta} + \tilde{d}_{w\xi}^T d_{w\xi} + \tilde{d}_{w\eta}^T d_{w\eta}$$

$$+ \frac{\tilde{m}_L \tilde{d}_{w\xi}^T (\bar{U} + la)}{m_Q + m_L}.$$

Consider the Lyapunov candidate function of the closed-loop system as:

$$V = V_1 + V_2.$$

The time derivative of V is given by

$$\dot{V} = -e_{\xi 1}^T c_1 e_{\xi 1} - e_{\xi 2}^T k_1 e_{\xi 2} - e_{\eta 1}^T c_2 e_{\eta 1} - e_{\eta 2}^T k_2 e_{\eta 2} - \tilde{d}_{w\xi}^T k_3 \tilde{d}_{w\xi}$$

$$- \tilde{d}_{w\eta}^T k_4 \tilde{d}_{w\eta}$$

$$- e_{\xi 2}^T \tilde{d}_{w\xi} - e_{\eta 2}^T \tilde{d}_{w\eta} + \tilde{d}_{w\xi}^T d_{w\xi} + \tilde{d}_{w\eta}^T d_{w\eta} + \frac{\tilde{m}_L \tilde{d}_{w\xi}^T (\bar{U} + la)}{m_Q + m_L}$$

$$+ \frac{\gamma_2 \tilde{m}_L \hat{m}_L (\bar{U} + la)^T (\bar{U} + la)}{\gamma_1 (m_Q + m_L)}. \tag{19}$$

Recalling Assumption 4 and Young inequality, it can be deduced that

$$-e_{\xi 2}^T \tilde{d}_{w\xi} \le \frac{e_{\xi 2}^T e_{\xi 2} + \tilde{d}_{w\xi}^T \tilde{d}_{w\xi}}{2},$$

$$-e_{\eta 2}^T \tilde{d}_{w\eta} \le \frac{e_{\eta 2}^T e_{\eta 2} + \tilde{d}_{w\eta}^T \tilde{d}_{w\eta}}{2},$$

$$\tilde{d}_{w\xi}^T d_{w\xi} \le \frac{\tilde{d}_{w\xi}^T \tilde{d}_{w\xi} + d_{w\xi}^2}{2} \le \frac{\tilde{d}_{w\xi}^T \tilde{d}_{w\xi} + E_{w\xi}^2}{2},$$

$$\tilde{d}_{w\eta}^T d_{w\eta} \le \frac{\tilde{d}_{w\eta}^T \tilde{d}_{w\eta} + d_{w\eta}^2}{2} \le \frac{\tilde{d}_{w\eta}^T \tilde{d}_{w\eta} + E_{w\eta}^2}{2},$$

$$\frac{\tilde{m}_L \tilde{d}_{w\xi}^T (\bar{U} + la)}{m_Q + m_L} \le \frac{\tilde{d}_{w\xi}^T \tilde{d}_{w\xi}}{2(m_Q + m_L)} + \frac{\tilde{m}_L^2 (\bar{U} + la)^T (\bar{U} + la)}{2(m_Q + m_L)}.$$

Substituting the above inequalities into Equation (19), it can be deduced that

$$\dot{V} \le -e_{\xi 1}^T c_1 e_{\xi 1} - e_{\xi 2}^T \left(k_1 - \frac{I}{2} \right) e_{\xi 2} - e_{\eta 1}^T c_2 e_{\eta 1} - e_{\eta 2}^T \left(k_2 - \frac{I}{2} \right) e_{\eta 2}$$

$$- \tilde{d}_{w\xi}^T (k_3 - MI) \tilde{d}_{w\xi} - \tilde{d}_{w\eta}^T (k_4 - I) \tilde{d}_{w\eta} + \frac{E_{w\xi}^2}{2} + \frac{E_{w\eta}^2}{2}$$

$$+ K \left(\gamma \tilde{m}_L \hat{m}_L + \frac{\tilde{m}_L^2}{2} \right),$$

where $M = 1 + \frac{1}{2(m_Q + m_L)}$, $K = \frac{(\bar{U} + la)^T (\bar{U} + la)}{m_Q + m_L}$, $\gamma = \frac{\gamma_2}{\gamma_1}$, and I is an identity matrix.

Furthermore, since the inequality $\tilde{m}_L \hat{m}_L = -\tilde{m}_L^2 + \tilde{m}_L m \le -\frac{\tilde{m}_L^2}{2} + \frac{m_L^2}{2}$ holds, we can conclude that

$$\dot{V} \le -e_{\xi 1}^T c_1 e_{\xi 1} - e_{\xi 2}^T \left(k_1 - \frac{I}{2} \right) e_{\xi 2} - e_{\eta 1}^T c_2 e_{\eta 1} - e_{\eta 2}^T \left(k_2 - \frac{I}{2} \right) e_{\eta 2}$$

$$- \tilde{d}_{w\xi}^T (k_3 - MI) \tilde{d}_{w\xi} - \tilde{d}_{w\eta}^T (k_4 - I) \tilde{d}_{w\eta} - \frac{K(\gamma - 1)}{2} \tilde{m}_L^2$$

$$+ \frac{K\gamma}{2} m_L^2 + \frac{E_{w\xi}^2}{2} + \frac{E_{w\eta}^2}{2}$$

$$\le -aV + b, \tag{20}$$

where $a = \min_{i \in \{1,2,3\}} \min\{c_{1i}, c_{2i}, k_{1i} - \frac{1}{2}, k_{2i} - \frac{1}{2}, k_{3i} - M, k_{4i} - 1, \frac{K(\gamma-1)}{2}\}$, $b = \frac{K\gamma}{2} m_L^2 + \frac{E_{w\xi}^2}{2} + \frac{E_{w\eta}^2}{2}$.

From Equation (20) we can obtain:

$$V(t) \le \frac{b}{a} + \left(V(t_0) - \frac{b}{a} \right) e^{-a(t - t_0)}, \forall t \ge t_0. \tag{21}$$

Based on Equation (21), if the control parameters satisfy that $k_{1i} > \frac{1}{2}$, $k_{2i} > \frac{1}{2}$, $k_{3i} > M$, $k_{4i} > 1$ ($i = 1, 2, 3$), and $\gamma > 1$, then there exists t' such that the error $e = e_{\xi 1}^T e_{\xi 1} + e_{\xi 2}^T e_{\xi 2} + e_{\eta 1}^T e_{\eta 1} + e_{\eta 2}^T e_{\eta 2} + \frac{\tilde{m}_L}{\gamma_1 (m_Q + m_L)} + \tilde{d}_{w\xi}^T \tilde{d}_{w\xi} + \tilde{d}_{w\eta}^T \tilde{d}_{w\eta}$ satisfies $e(t) \le \frac{2b}{a}$ when $t > t'$.

This completes the proof. □

Remark 3. In terms of parameters selection, choosing larger values of k_i ($i = 1, 2, 3, 4$) in the controller reduces the error e, but also increases the energy consumption. In the adaptive control law, larger values of γ_1 and γ_2 can result in more accurate estimation and faster convergence time. However, larger values also introduce the problem of chattering. Therefore, it is important to choose the control parameters appropriately.

5 | SIMULATION

In this section, simulations are conducted to demonstrate the effectiveness and robustness of the designed controller. The physical parameters are listed in Table 1, and the drag
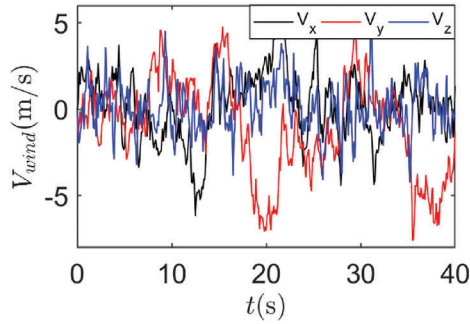
FIGURE 3 The Dryden wind.

TABLE 1 Physical parameters.

Parameter	Value	Unit	Parameter	Value	Unit
g	9.81	m/s^2	I_x	3×10^{-2}	kg m^2
m_Q	1.8	kg	I_y	3×10^{-2}	kg m^2
l	1.5	m	I_z	3×10^{-2}	kg m^2

TABLE 2 Wind disturbance coefficient.

Control loop	Wind disturbance coefficient
ξ	$\lambda_{11} = 0.4, \lambda_{12} = 0.4, \lambda_{13} = 0.4$
η	$\lambda_{21} = 0.1, \lambda_{22} = 0.2, \lambda_{23} = 0.1$
σ	$\lambda_{31} = 0.0025, \lambda_{32} = 0.0025$

TABLE 3 Parameters of controllers.

Controllers	Parameters and values
U	$c_{11} = 1, c_{12} = 1, c_{13} = 2, k_{11} = 1, k_{12} = 1, k_{13} = 2, \gamma_1 = 0.3, \gamma_2 = 0.5$
τ	$c_{21} = 2, c_{22} = 2, c_{23} = 1, k_{11} = 2, k_{12} = 2, k_{13} = 1$
Disturbance observers	$k_{31} = 20, k_{32} = 20, k_{33} = 20, k_{41} = 7, k_{42} = 7, k_{43} = 7$

coefficients are provided in Table 2. The control parameters are given in Table 3.

The wind speed at a height of 6.096 m is taken to be 10 m/s. The generated Dryden wind according to Equations (7) and (8) is shown in Figure 3.

Three scenarios are presented in this section. The first scenario involves the comparison between the performance of the designed disturbance observer, the adaptive disturbance observer, and no disturbance observer under the wind disturbance. In the second scenario, the designed adaptive controller with a convergence term is compared with an adaptive control strategy without a convergence term. In the third scenario, the performance of the controller designed in this paper is compared with the two previous control strategies as well as SMC. These scenarios are made to verify the effectiveness and superiority of the proposed controller. The initial conditions
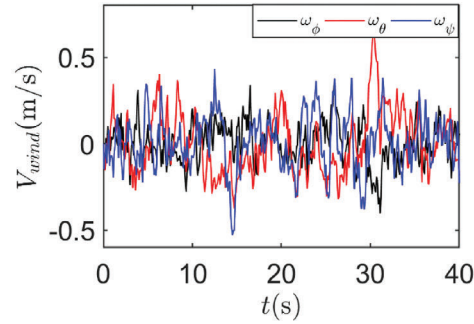
TABLE 4 Maximum tracking error.

	Designed disturbance observer	Adaptive disturbance observer	No disturbance observer
x	0.0493 m	0.6267 m	1.6932 m
y	0.0814 m	0.7447 m	3.7352 m
z	0.0123 m	0.2543 m	0.1548 m
ψ	0.0021 rad	0.0689 rad	0.3642 rad

of the system are chosen as $\xi_0 = [0, 0, 0]^T$, $\sigma_0 = [0, 0]^T$, $\eta_0 = [0, 0, 0]^T$. The desired trajectory ξ_d and the desired yaw angle ψ_d are set as $\xi_d = [\sin t, \cos t, 2 + 0.1t]^T$ m, $\psi_d = 2$ rad.

5.1 | Scenario 1

In the first scenario, only the effect of wind disturbance on quadrotor suspended load system is considered. The trajectory tracking is shown in Figure 4, which compares the performance of the controller with the designed disturbance observers, the adaptive disturbance observers, and the no disturbance observers. The adaptive disturbance observers are as follows:

$$\dot{\hat{d}}_{w\xi} = -\delta_1 e_{\xi 2},$$

$$\dot{\hat{d}}_{w\eta} = -\delta_2 e_{\eta 2}.$$

where $\delta_1 = \text{diag}(\delta_{11}, \delta_{12}, \delta_{13})$, $\delta_2 = \text{diag}(\delta_{21}, \delta_{22}, \delta_{23})$ are positive definite.

The estimation errors of the designed disturbance observer and the adaptive disturbance observer are shown in Figure 5. The tracking errors of the three controllers are listed in Table 4. It is evident that wind disturbances have a significant impact on the quadrotor suspended load system. Without the disturbance observers, the system displays large tracking errors. However, with the addition of the disturbance observers, the tracking errors are significantly lowered. Moreover, it can be seen that the designed disturbance observer outperforms the adaptive disturbance observer in addressing the wind disturbance. Figure 5 further demonstrates the superiority of the
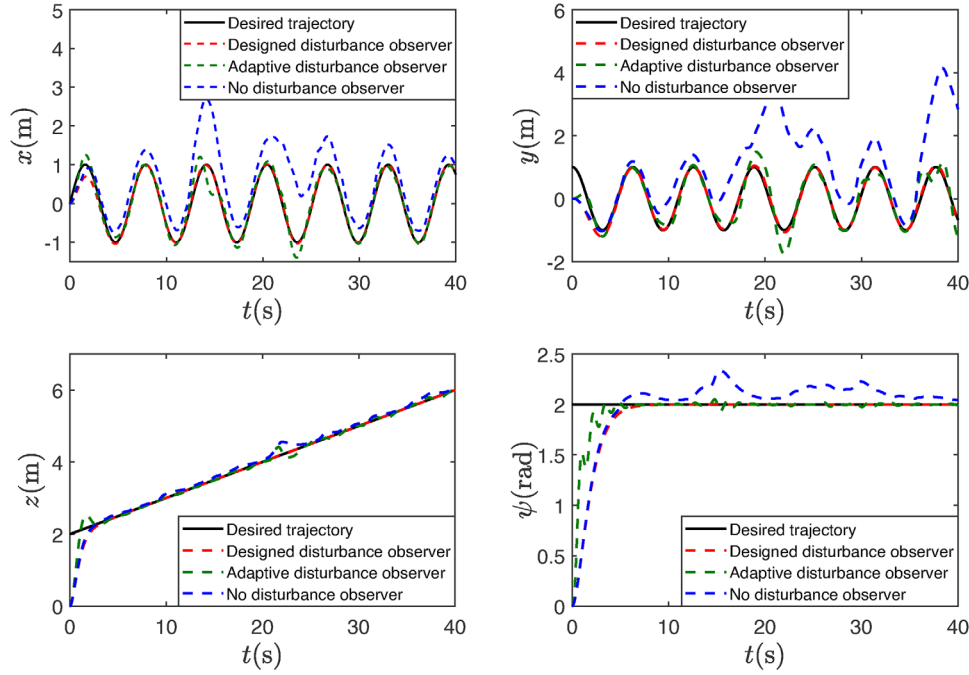
FIGURE 4   Trajectory tracking in the presence of wind disturbances.
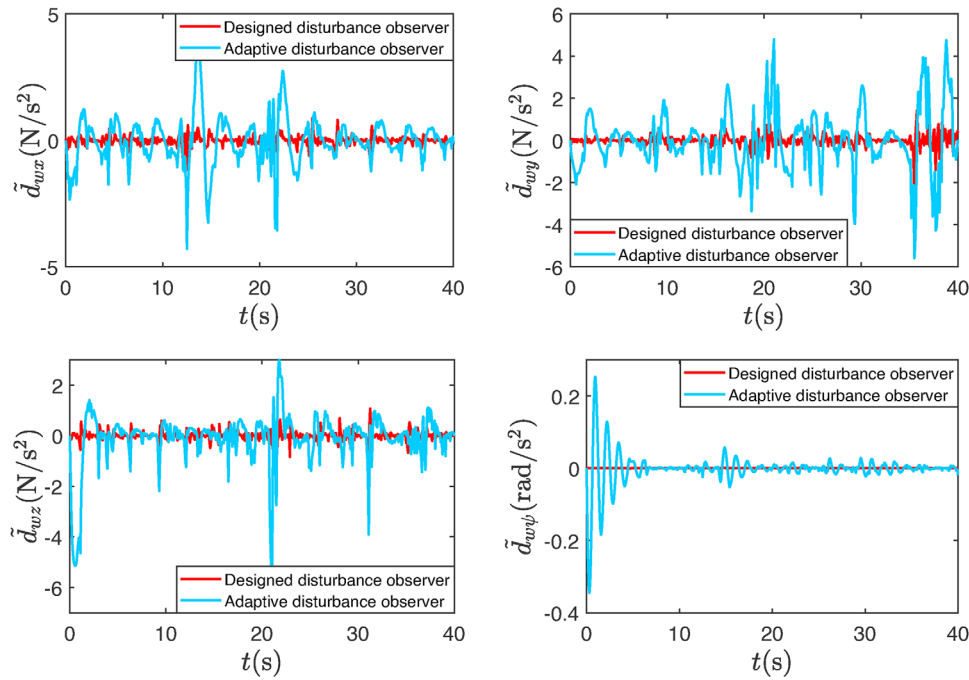

FIGURE 5   The estimation errors of two disturbance observers.

designed disturbance observer against strong and irregular wind disturbances. In comparison to the adaptive disturbance observer, the designed disturbance observers can estimate the wind disturbances more accurately, showing smaller estimation errors.

The simulation results show that the application of the disturbance observer significantly improves the performance of the quadrotor suspended load system under wind disturbance,

reduces the tracking error, and enhances the robustness of the system.

5.2 | Scenario 2

In the second scenario, the impact of different payloads on trajectory tracking performance is investigated. To simulate the
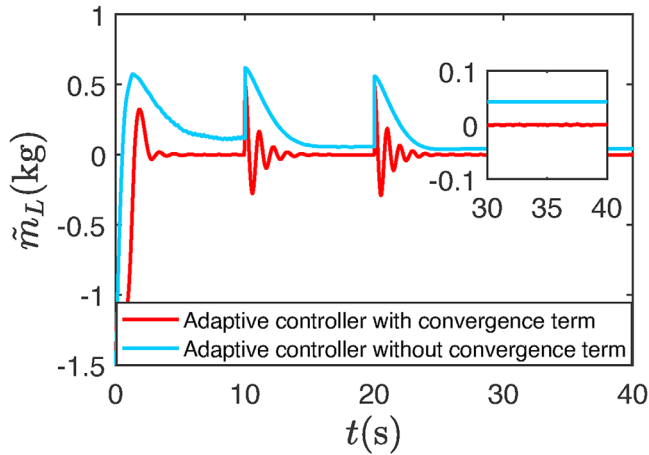
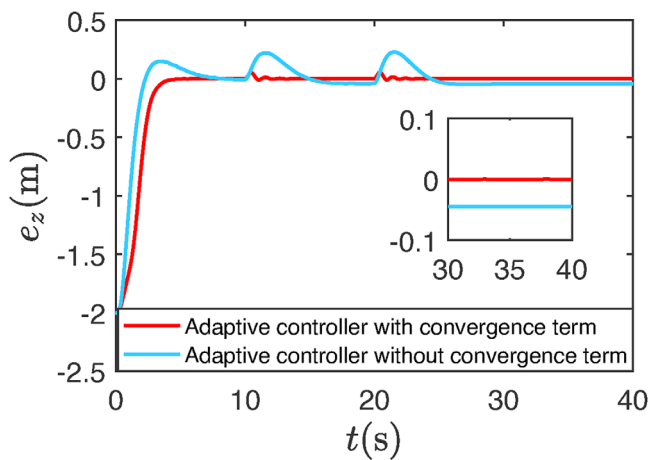**FIGURE 6** Mass estimation error of payload.

FIGURE 7 The altitude tracking errors.

uncertainties generated by the payload, the variation of payload is assumed to be as:

$$m_L = \begin{cases} 1.5, & t \in [0, 10), \\ 1, & t \in [10, 20), \\ 0.5, & t \in [20, 40]. \end{cases}$$

This subsection compares two adaptive control strategies. One contains a convergence term as described in Equation (13), and the other does not. The control law without the convergence term is as follows:

$$\dot{\hat{m}}_L = \gamma_1 e_{\xi2}^T (\bar{U} + la).$$

The comparison of the two strategies in estimation error is illustrated in Figure 6. As payload mass has a significant effect on the altitude of the quadrotor, this subsection only presents the altitude tracking errors under the two adaptive control laws. The results are shown in Figure 7. It can be observed that

the adaptive control law with the convergence term has better performances. The strategy proposed in this paper brings the estimation error to zero and the accuracy is improved. This result confirms the superiority of the adaptive control strategy proposed in this paper.

5.3 | Scenario 3

In the third subsection, the effects of wind disturbances and payload mass variations on the system are considered together. To demonstrate the effectiveness of the designed control strategy, we compare it with the adaptive disturbance observer combined with the convergence-free term adaptive law (ADOA), and the SMC.

Figure 8 shows the swing angles with all three controllers, the payload swings with a small magnitude with both the designed controller and SMC, but it swings with a large magnitude with ADOA. Trajectory tracking of the quadrotor with all three controllers is shown in Figure 9. It is clear that SMC fails to follow the desired trajectory when the payload changes, whereas both the designed controller and ADOA successfully track the desired trajectory. At the same time, the designed controller shows better tracking performance compared to ADOA. The tracking errors of all three controllers are shown in Figure 10. In the presence of variable payload and wind disturbances, the designed controller exhibits smaller tracking errors and better stability compared to ADOA and SMC. Figure 11 shows the estimation of the disturbance observer and adaptive law in the presence of both payload mass variations and wind disturbance. The results indicate that there is some bias in the estimation of actual values due to the interaction caused by their coupling. However, the system is still able to track the desired trajectory accurately, which shows that the control strategy remains effective even under payload variations and wind disturbances.

In conclusion, compared to ADOA and SMC, the designed control method demonstrates enhanced resilience to disturbances, accurately estimates payload mass variations despite wind disturbances, and enables quadrotor suspended payload systems to achieve rapid and precise trajectory tracking with small swing angles.

6 | CONCLUSION

This paper has presented an adaptive control scheme based on disturbance observers for quadrotor suspended payload systems. In this control scheme, adaptive controller and disturbance observers have been employed to estimate the payload mass and wind disturbance, respectively. The uniform boundedness of all error signals has been demonstrated. Additionally, the Dryden model has been developed to simulate real wind disturbances. Finally, simulations have been conducted to verify the effectiveness of the designed controller. Future work will focus on conducting outdoor experiments and developing adaptive fuzzy tracking control of quadrotor suspended load systems.
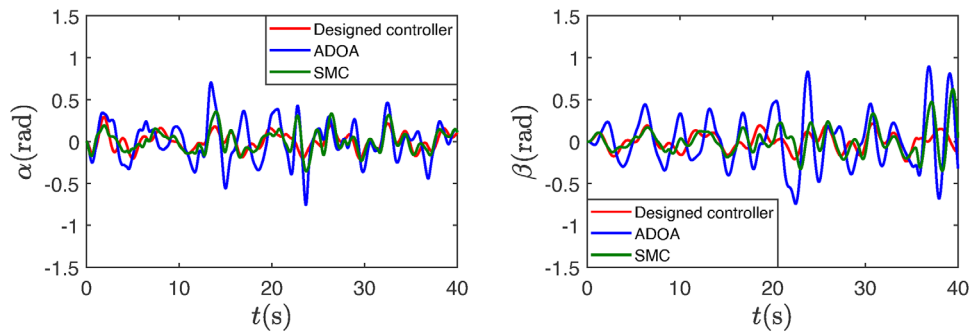
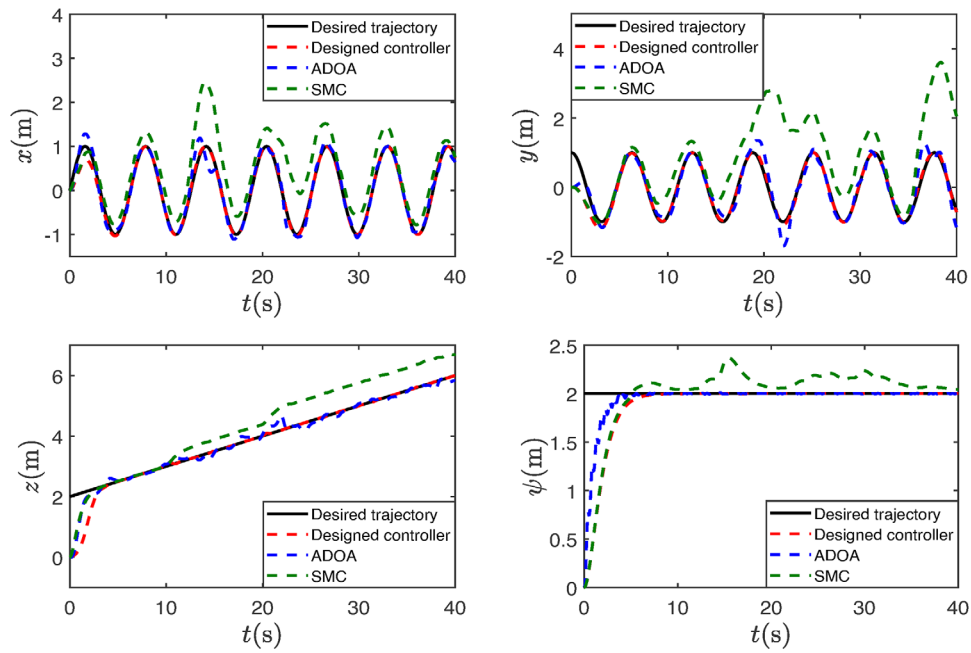**FIGURE 8** Swing angles in the presence of payload variations and wind disturbances.

FIGURE 9 Trajectory tracking in the presence of payload variations and wind disturbances.
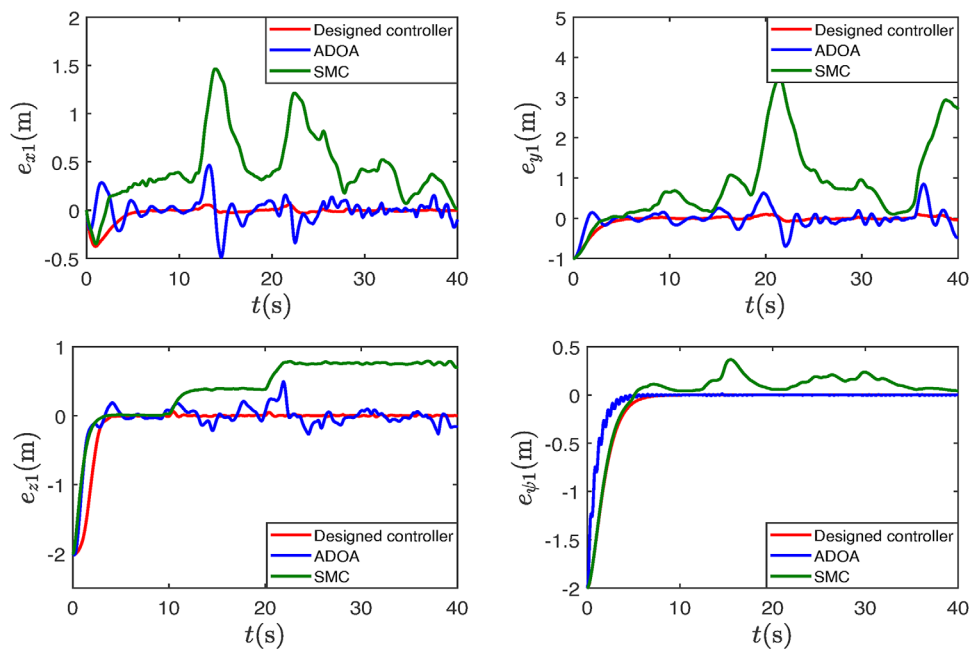

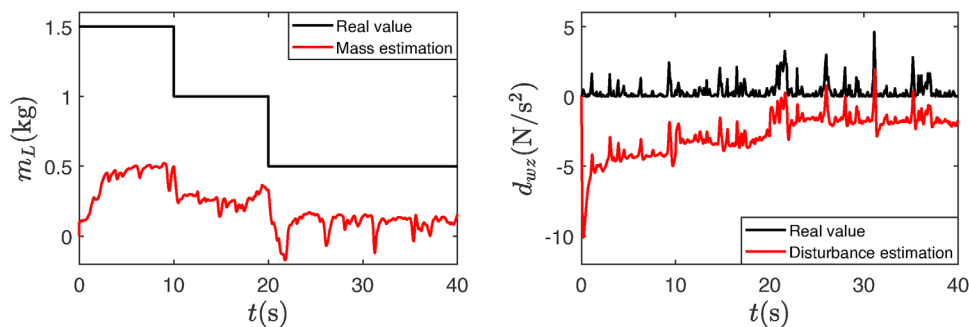**FIGURE 10** Trajectory errors in the presence of payload variations and wind disturbances.

FIGURE 11   The estimation of the disturbance observer and adaptive law.

AUTHOR CONTRIBUTIONS

Ruiying Wang: Investigation; methodology; software; writing—original draft. **Jun Shen**: Funding acquisition; project administration. **Hongling Qiu**: Conceptualization; supervision; editing. **Bohao Zhu**: Project administration; supervision.

ACKNOWLEDGEMENTS

CONFLICT OF INTEREST STATEMENT

The authors declare no conflicts of interest.

DATA AVAILABILITY STATEMENT

Data sharing not applicable to this article as no datasets were generated or analyzed during the current study.

ORCID

Ruiying Wang https://orcid.org/0009-0005-4702-8806
Hongling Qiu https://orcid.org/0000-0001-8698-8811
Bohao Zhu https://orcid.org/0000-0002-6431-7395

REFERENCES

1. Goodarzi, F., Lee, D., Lee, T.: Geometric control of a quadrotor UAV transporting a payload connected via flexible cable. Int. J. Control Autom. Syst. 13, 1486–1498 (2015)
2. Tang, S., Wüest, V., Kumar, V.: Aggressive flight with suspended payloads using vision-based control. IEEE Rob. Autom. Lett. 3(2), 1152–1159 (2018)
3. Wang, J., Yuan, X., Zhu, B.: Geometric control for trajectory-tracking of a quadrotor UAV with suspended load. IET Control Theory Appl. 16(12), 1271–1281 (2022)
4. Palunko, I., Cruz, P., Fierro, R.: Agile load transportation: safe and efficient load manipulation with aerial robots. IEEE Rob. Autom. Mag. 19(3), 69–79 (2012)
5. Qian, L., Liu, H.: Dynamics and control of a quadrotor with a cable suspended payload. In: 30th Canadian Conference on Electrical and Computer Engineering, CCECE, pp. 1–4. IEEE, Piscataway, NJ (2017)
6. Yang, S., Xian, B.: Trajectory tracking control design for the system of a quadrotor UAV with a suspended payload. In: 36th Chinese Control Conference, CCC, pp. 777–782. IEEE, Piscataway, NJ (2017)
7. Godbole, A.R., Subbarao, K.: Mathematical modeling and control of an unmanned aerial system with a cable suspended payload. In: 2018 IEEE 14th International Conference on Control and Automation, ICCA, Anchorage, AK, USA, pp. 570–575. IEEE, Piscataway, NJ (2018)
8. Guerrero, M., Mercado, D., Lozano, R., García, C.: Swing-attenuation for a quadrotor transporting a cable-suspended payload. ISA Trans. 68, 433–449 (2017)
9. Lee, T.: Geometric control of quadrotor UAVs transporting a cable-suspended rigid body. IEEE Trans. Control Syst. Technol. 26(1), 255–264 (2017)
10. Yu, G., Cabecinhas, D., Cunha, R., Silvestre, C.: Nonlinear backstepping control of a quadrotor-slung load system. IEEE/ASME Trans. Mechatron. 24(5), 2304–2315 (2019)
11. Cruz, P., Fierro, R.: Cable-suspended load lifting by a quadrotor UAV: Hybrid model, trajectory generation, and control. Auton. Rob. 41, 1629–1643 (2017)
12. Lee, T.: Robust adaptive attitude tracking on $SO(3)$ with an application to a quadrotor UAV. IEEE Trans. Control Syst. Technol. 21(5), 1924–1930 (2012)
13. Mofid, O., Mobayen, S.: Adaptive sliding mode control for finite-time stability of quadrotor UAVs with parametric uncertainties. ISA Trans. 72, 1–14 (2018)
14. Liu, Y., Ou, T.: Non-linear adaptive tracking control for quadrotor aerial robots under uncertain dynamics. IET Control Theory Appl. 15(8), 1126–1139 (2021)
15. Yang, S., Xian, B.: Energy-based nonlinear adaptive control design for the quadrotor UAV system with a suspended payload. IEEE Trans. Ind. Electron. 67(3), 2054–2064 (2019)
16. Ha, C., Zuo, Z., Choi, F., Lee, D.: Passivity-based adaptive backstepping control of quadrotor-type UAVs. Rob. Auton. Syst. 62(9), 1305–1315 (2014)
17. Sumantri, B., Uchiyama, N., Sano, S.: Least square based sliding mode control for a quadrotor helicopter and energy saving by chattering reduction. Mech. Syst. Sig. Process. 66, 769–784 (2016)
18. Wang, B., Yu, X., Mu, L., Zhang, Y.: Disturbance observer-based adaptive fault-tolerant control for a quadrotor helicopter subject to parametric uncertainties and external disturbances. Mech. Syst. Sig. Process. 120, 727–743 (2019)
19. Xu, G., Xia, Y., Zhai, D., Cui, B.: Adaptive sliding mode disturbance observer–based funnel trajectory tracking control of quadrotor with external disturbances. IET Control Theory Appl. 15(13), 1778–1788 (2021)
20. Shao, X., Liu, J., Wang, H.: Robust backstepping output feedback trajectory tracking for quadrotors via extended state observer and sigmoid tracking differentiator. Mech. Syst. Sig. Process. 104, 631–647 (2018)
21. Sini, S., Ananthan, T.: A disturbance observer based control for quadrotor aircraft subject to wind gusts. In: 2022 IEEE International Conference on Signal Processing, Informatics, Communication and Energy Systems (SPICES), vol. 1, pp. 491–496. IEEE, Piscataway, NJ (2022)
22. Wang, C., Song, B., Huang, P., Tang, C.: Trajectory tracking control for quadrotor robot subject to payload variation and wind gust disturbance. J. Intell. Rob. Syst. 83, 315–333 (2016)
23. Guerrero, M., Lozano, R., Castillo, P., Hernández, O., García, C., Valencia, G.: Nonlinear control strategies for a UAV carrying a load with swing attenuation. Appl. Math. Modell. 91, 709–722 (2021)

24. Hancer, C., Oner, K., Sirimoglu, E., Cetinsoy, E., Unel, M.: Robust position control of a tilt-wing quadrotor. In: 49th IEEE Conference on Decision and Control, CDC, pp. 4908–4913. IEEE, Piscataway, NJ (2010)

25. Qian, L., Liu, H.: Path-following control of a quadrotor UAV with a cable-suspended payload under wind disturbances. IEEE Trans. Ind. Electron. 67(3), 2021–2029 (2019)

26. Lv, Z., Wu, Y., Rui, W.: Nonlinear motion control for a quadrotor transporting a cable-suspended payload. IEEE Trans. Veh. Technol. 69(8), 8192–8206 (2020)

27. Lv, Z., Li, S., Wu, Y., Wang, Q.: Adaptive control for a quadrotor transporting a cable-suspended payload with unknown mass in the presence of rotor downwash. IEEE Trans. Veh. Technol. 70(9), 8505–8518 (2021)

28. Mohammadi, A., Marquez, H., Tavakoli, M.: Nonlinear disturbance observers: design and applications to Euler Lagrange systems. IEEE Control Syst. Mag. 37(4), 50–72 (2017)